CHAPTER IV

EFFECT OF SURFACE MODIFIED BOVINE BONE BASED HYDROXYAPATITE ON PHYSICAL PROPERTIES AND *in vitro* CYTOTOXICITY OF HA/PLA COMPOSITES

4.1 Abstract

In this work, hydroxyapatite (HA) was produced from bovine bone in order to use as a filler for poly(lactic acid) (PLA) composites. The surface of HA powder was modified with either 3-aminopropyltriethoxysilane (APES) or 3-methacryloxypropyl trimethoxysilane (MPTS). FTIR and EDXRF results confirmed the appearance of APES and MPTS on the HA surfaces. SEM micrographs of silane-treated HA/PLA composites revealed that modification of HA with APES or MPTS eased distribution of HA powder in PLA matrix and enhanced interfacial adhesion between both phases. Based on the results, the mechanical properties of silane-treated HA/PLA composites were better than those of untreated HA/PLA composites. In addition, *in vitro* cytotoxicity tests indicated that the extracts from all HA/PLA composites had no toxicity to human osteoblast cell.

4.2 Introduction

Hydroxyapatite [HA: $Ca_{10}(PO_4)_6(OH)_2$] is a form of calcium phosphate which is similar to a major mineral phase in hard tissues of human body. HA has been found to be an application as a biomaterial because of its excellent biocompatibility and bone-bonding ability. It has been used in various medical applications such as bone replacement (Kothapalli *et al.*, 2005; Shikinami *et al.*, 2001; Hasegawa *et al.*, 2006; Fathi *et al.*, 2008). HA can be synthetically prepared or derived from natural sources, *e.g.* coral, bovine bone, swine bone. In recent years, several attempts have been done to produce HA from natural sources for biomedical applications since the natural HA is less expensive and more compatible to human hard tissues (Benmarouane *et al.*, 2004, Ruksudjarit *et al.*, 2008; Yoganand *et al.*, 2009). In Thailand, bovine bone as a livestock waste is normally used in fertilizer, animal foods, and in making porcelain (*i.e.* bone china). Using the bovine bone as a raw material for producing HA is not only to reduce volumes of the livestock waste but also to increase added value of the bovine bone. However, HA is brittle and difficult to process into required shapes. One attempt to solve this problem is mixing HA with a flexible polymer, especially with a bioresorbable polymer.

Many kinds of bioresorbable polymers, *e.g.* poly(lactic acid) (PLA), poly(3-hydroxybutyrate) (PHB), have been developed and used in medical applications. Among those polymers, PLA is a good candidate as a biomaterial due to its biocompatibility, biodegradability and yielding nontoxic byproducts after hydrolysis reaction (Deng *et al.*, 2001; Ignjatovic *et al.*, 2001). Hence, a composite between PLA and HA is a good alternative for using as a biomaterial since it combines strength and

stiffness of HA with flexibility and resorbability of PLA and, then, solving the drawbacks of both materials (Russias *et al.*, 2006; Tsuji *et al.*, 2004).

However, the major drawbacks found in HA/PLA composites are the agglomeration of HA and the failure at the interface between HA and the polymer matrix. These are due to the polarity difference between PLA matrices and HA surfaces. PLA matrix has methyl groups ($-CH_3$) as side group of a polymer chain and, thus, PLA surface shows hydrophobicity. This is in contrast to HA surface which exhibits hydrophilic property (Shikinami *et al*., 2001; Liu *et al.*, 1998; Zhang *et al.*, 2005). Based on mechanical properties of HA/PLA composites, an improvement of the interfacial adhesion between HA particles and PLA matrix has become an important area of studies. The HA surface can be modified with a coupling agent, such as organofunctional silanes, by which the interfacial adhesion between filler and polymer matrix is effectively improved (Russias *et al.*, 2006; Dupraz *et al.*, 1996).

In this present study, bovine bone based HA was prepared and was treated with 3-aminopropyltriethoxysilane (APES) or 3-methacryloxypropyltrimethoxysilane (MPTS), and then incorporated into PLA. The characteristics of untreated HA and silane-treated HA were investigated. In addition, effects of filler characteristic and filler content on morphological and mechanical properties of HA/PLA composites were determined. Furthermore, *in vitro* cytotoxicity of the HA/PLA composites was also investigated.

4.3 Experimental

4.3.1 Materials

PLA (4042D) was purchased from NatureWorks LLC Co. Ltd. Bovine bones were supplied by Limeiseng Co., Nakhon Ratchasima, Thailand. 3-aminopropyltriethoxysilane (APES) and 3-methacryloxypropyltrimethoxysilane (MPTS) were purchased from Optimal Tech Co.,Ltd. and Aldrich, respectively. Chemical structures of these silane coupling agents are shown in Figure 4.1.

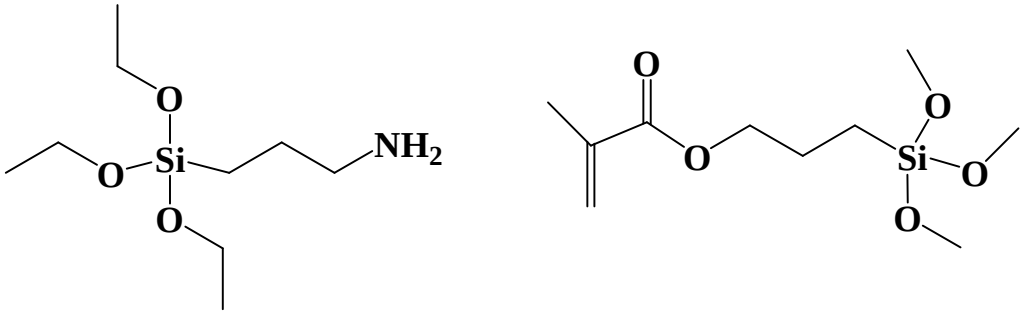

(a) **(b)**

Figure 4.1 Chemical structures of (a) 3-aminopropyltriethoxysilane and (b) 3-methacryloxypropyltrimethoxysilane.

4.3.2 Preparation of HA powder

Bovine bones were burned in open air and ground into powder using a ball milling machine. Then, the powder was heat treated at 1100ºC for 3 h; the obtained powder was called untreated HA (u-HA). After that, the powder was modified by either APES or MPTS. The content of silane used for modification was 2.0wt% based on weight of HA powder. To prepare silane solution, the APES was dissolved in distilled water whereas MPTS was dissolved in 30vol.% of alcoholic solution. The pH of each silane solution was adjusted to 3.5 using acetic acid. HA powder was soaked in each silane solution and left under agitation at room temperature. After 3 h of agitation, the pH of each solution was increased to 7.0 with 0.1 N NaOH solution to encourage condensation and formation of siloxanols on HA surface (Ooi *et al.*, 2007). Then, both silane-treated powders were washed and dried at 60ºC overnight in an oven. The APES treated HA and MPTS treated HA were designated as a-HA and m-HA, respectively.

4.3.3 Preparation of HA/PLA composites

HA/PLA composites were prepared through melt-mixing technique using an internal mixer (HAAKE/RHEOMIX). PLA and HA were mixed at 170ºC with a rotor speed of 70 rpm for 10 min. The weight ratios of HA/PLA in each composite are shown in Table 4.1. Each HA/PLA composite was left at room temperature for 24 h before grinding into small pieces. To prepare composite specimens for mechanical tests, the ground HA/PLA composite was heated in dumbbell-shaped and rectangular-shaped molds from room temperature to 180ºC and maintained at that temperature for 10 min. Subsequently, it was hot-pressed vertically for 5 min at 180ºC under a pressure of 1.4×10^7 Pa and cooled to room temperature.

Table 4.1 Composition of HA/PLA composites.

Composite designations	Filler	Silane coupling	Filler content (wt%)
1A	u-HA	-	10
2A	u-HA	-	20
3A	u-HA	-	30
4A	u-HA	-	40
1B	a-HA	APES	10
2B	a-HA	APES	20
3B	a-HA	APES	30
4B	a-HA	APES	40
1C	m-HA	MPTS	10
2C	m-HA	MPTS	20
3C	m-HA	MPTS	30
4C	m-HA	MPTS	40

4.3.4 Characterization of HA powder

Functional groups of u-HA, m-HA and a-HA powders were identified by a Fourier transform infrared spectrometer (FTIR) (BIO-RAD/FTS175C, diffuse reflectance technique) in the 4000-400 cm^{-1} region with 2 cm^{-1} resolution.

Elemental compositions of the u-HA, m-HA and a-HA powders were analyzed by an energy dispersive X-Ray fluorescence spectroscopy (EDXRF) (OXFORD/ED2000). EDXRF measurements were carried out with a rhodium lamp (energy range 10^4 eV). The X-ray tube was operated at 5.0 kV, the pulse rate was kept

at 20 kcps and the measurement resolution was kept at 170 eV. Each peak of the recorded spectrum is a characteristic of a particular element.

In addition, a scanning electron microscopy (SEM) (JOEL/JSM-6400) operating at 15-20 kV was used to reveal microstructures of u-HA, m-HA and a-HA powders. Median particle sizes of u-HA, m-HA and a-HA powders were measured by a diffraction particle analyzer (MASTERSIZER S/MSS).

4.3.5 Characterization of HA/PLA composites

A scanning electron microscopy (SEM) (JOEL/JSM-6400) operating at 20 kV was used to visualize tensile fracture surfaces of the HA/PLA composites. All samples were coated with a thin layer of gold before examination. Tensile properties of HA/PLA composites were investigated according to ASTM D638-03 using a universal testing machine (INSTRON/5569). Moreover, izod impact strength of unnotched HA/PLA specimen was determined according to ASTM D256 using an impact testing machine (ATLAS/BPI).

4.3.6 Cytotoxicity of HA/PLA composites

Cytotoxicity of HA/PLA composites was determined based on a procedure modified from ISO 10993-5:1999(E) (test on extracts) using assessment of cell damage by morphological means. Human osteoblasts were used as cultured cells. Dulbecco's modified eagle medium (DMEM), complete medium supplemented with 10% horse serum, was used as a culture medium and an extraction vehicle. The culture medium was prepared under sterile condition to prevent microbial inflection. The pH of medium was maintained in a range of 7.2-7.4. HA/PLA composite specimens for the cell tests, *i.e.* 4A, 4B and 4C, were sterilized by ethylene oxide gas. Under an aseptic environment, the sterilized HA/PLA composite specimens were then

extracted by DMEM with an extraction ratio of 3.18 cm^2/ml using roller mixers at 37±2ºC for 24±2 h. The media without test specimen (the blank cultured media), subjected to the same extraction condition, was used as a reagent control. Thermanox (Nunc) coverslip and polyurethane film containing 0.1% zinc diethyldithiocarbamate (ZDEC) were used as a negative control material and a positive control material, respectively. The extracts were then filtered by 0.22 micron membrane filter prior to test. For cytotoxic determination, h-OBs of 45,000 cells/ml with either the control or a specimen extract were incubated in a 95±5% humidified atmosphere with 5±0.1% CO_2 at 37±2ºC for 24 h. After the cell culture experiments, the cells were stained with neutral red for the cell viability assay. The morphologies of cells were determined using a trinocular phase contrast microscope.

4.4 Results and discussion

4.4.1 Characterization of HA powder

FTIR spectrum of u-HA is shown in Figure 4.2 (a). The peaks at 1085, 1036, 963, 600 and 575 cm^{-1} were assigned to different vibration modes of PO_4^{3-} group in HA powder. The stretching and the bending vibration of structural OH groups in the apatite lattice were observed at 3571 cm^{-1} and 632 cm^{-1}, respectively. Additionally, vibrational peaks corresponding to CO_3^{2-} groups were also observed at 1457, 1411 and 878 cm^{-1} (Fathi *et al.*, 2008; Ooi *et al.*, 2007). FTIR pattern indicated that the calcined bovine bone powder was carbonated HA. The appearance of carbonate functional groups on surface of the obtained powder could be explained as follows: 1) During heating process, adsorbed carbon from atmosphere substituted the PO_4^{3-} groups of the HA or 2) The incompletely pyrolyzed carbon dissolved into the hydroxyapatite crystal (Ooi *et al*., 2007; Shinzato *et al.*, 2001; Furuzono *et al.*, 2001; Wen *et al.*, 2008). Figure 2 (b-c) shows FTIR spectra of the silane-treated HA powders. The additional peaks, compared with FTIR spectrum of u-HA, were observed. The peaks around 2950-2850 cm^{-1} were C−H stretching vibration of carbon chains of APES and MPTS deposited on HA surface. Also, the peak at 1080 cm^{-1} was attributed to the Si-O stretching vibration of both silane coupling agents. Additionally, FTIR spectrum of m-HA showed C=O stretching vibration of the deposited MPTS at 1712 cm^{-1} (Kothapalli *et al*., 2005; Liu *et al*., 1998; Wen *et al*., 2008; Bleach, Nazhat, Tanner, Kellomaki, and Tormala, 2002).

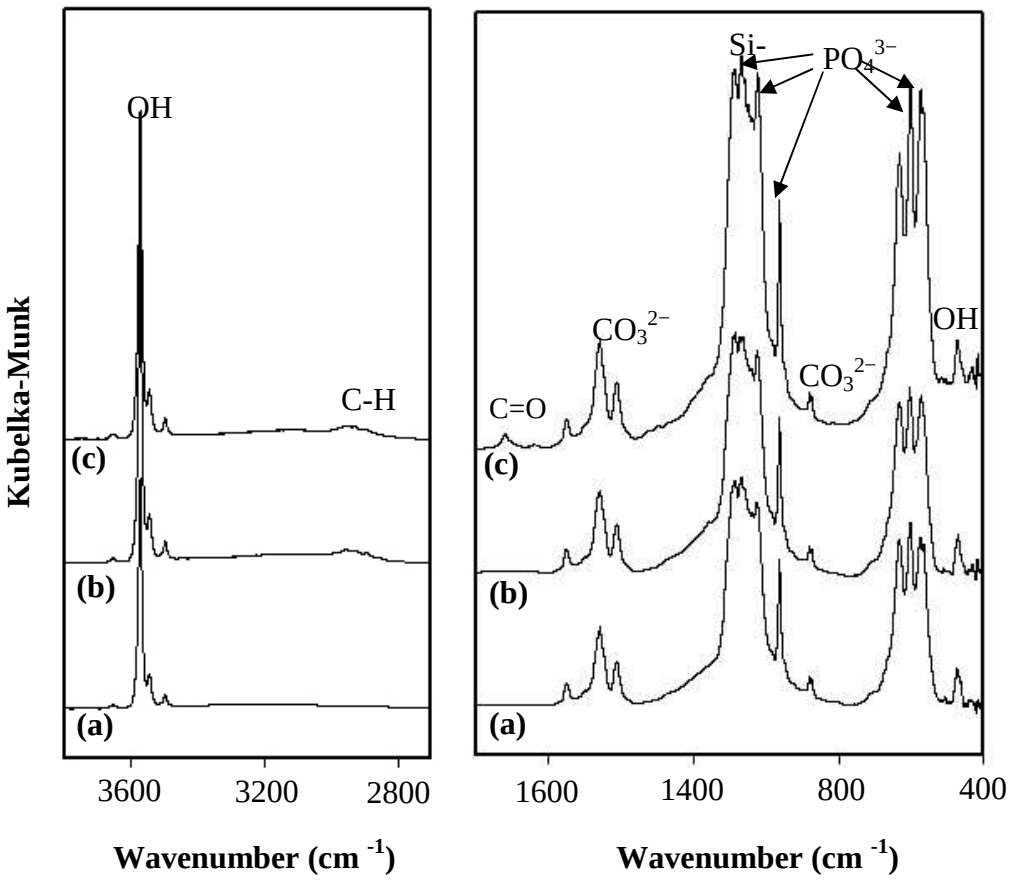

Figure 4.2 FTIR spectra of (a) u-HA, (b) a-HA and (c) m-HA.

Elemental compositions on the surfaces of u-HA, a-HA and m-HA are shown in Table 4.2 The major elements found on the u-HA surface were Ca and P, however, small amounts of Si were also observed. These Si atoms may come from impurity in raw material. In comparison between silane-treated HA and u-HA powders, the EDXRF results of a-HA and m-HA powders shows higher content of Si atoms on the powder surface. These results indicated the presence of silane molecules on the surface of the treated HA powders. This was a positive factor which could provide effective adhesion between PLA matrix and silane-treated HA powder. However, the percentage of the silane deposited on HA surface depended on silane

coupling type as shown in Table 4.2 According to another research group, parts of primary amino silane would be easier removed by rinsing with organic solvent or water than those of metacryloxy silane (Zhang *et al*., 2005).

Table 4.2 Elemental composition and median particle size of untreated HA and silane-treated HA.

Designation	**Elemental composition (%)**				**Median particle size (μm) (D (*v*, 0.5))**
	Ca	**P**	**O**	**Si**	
u-HA	25.5	11.5	62.2	0.06	14.30
a-HA	24.2	11.3	63.9	0.11	4.76
m-HA	23.6	11.0	64.5	0.13	4.53

In addition, SEM micrographs of u-HA, a-HA and m-HA are shown in Figure 4.3 (a-c). The micrographs in Figure 4.3 (a) shows the agglomeration of u-HA powder. On the other hand, the micrographs of silane-treated HA in Figure 4.3 (b) and (c) show the smaller sizes of agglomerated HA powders compared with those of u-HA. From the SEM observation, the agglomeration sizes of u-HA, a-HA and m-HA were consistent with their average particle size measured by the particle size analyzer (Table 4.2). These results indicated that silane surface treatment tended to reduce the agglomeration of HA powders. In preparation of HA/PLA composites, the less powder agglomeration would lead to better processibility and, accordingly, enhance mechanical properties of the composites.

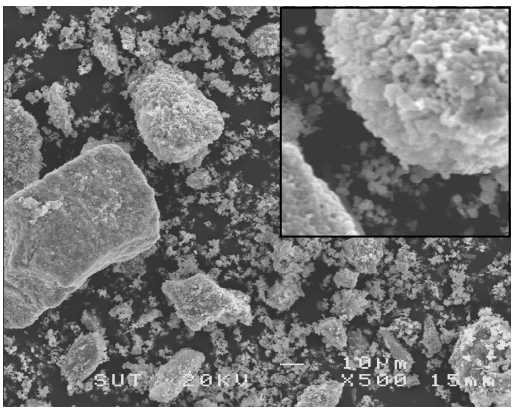

(a)

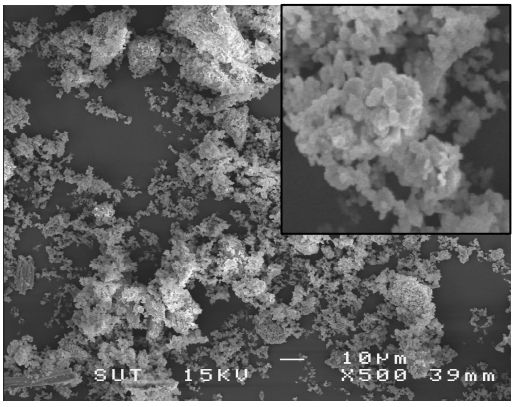

(b)

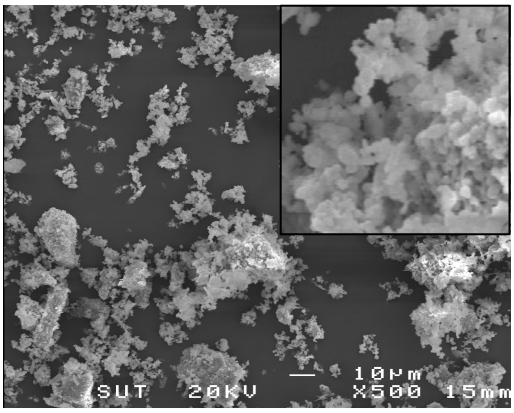

(c)

Figure 4.3 SEM micrographs of HA powders: (a) u-HA, (b) a-HA and (c) m-HA.

4.4.2 Characterization of HA/PLA composites

Tensile modulus, elongation at break, tensile strength and impact strength of HA/PLA composites at various HA contents are illustrated in Figure 4.4-4.7. As seen in the figures, the mechanical properties of silane-treated HA/PLA composites were better than those of untreated HA/PLA composites of the equal HA content.

Tensile moduli of HA/PLA composites were higher than that of the neat PLA as shown in Figure 4.4. Also, the tensile moduli of the composites increased

with increasing HA content. The stiffness enhancement of the HA/PLA composites was because the rigid HA filler restricts the molecular motion and the deformation of the PLA chains. At an equal content of filler, the tensile moduli of both a-HA/PLA and m-HA/PLA were slightly higher than that of u-HA/PLA composites.

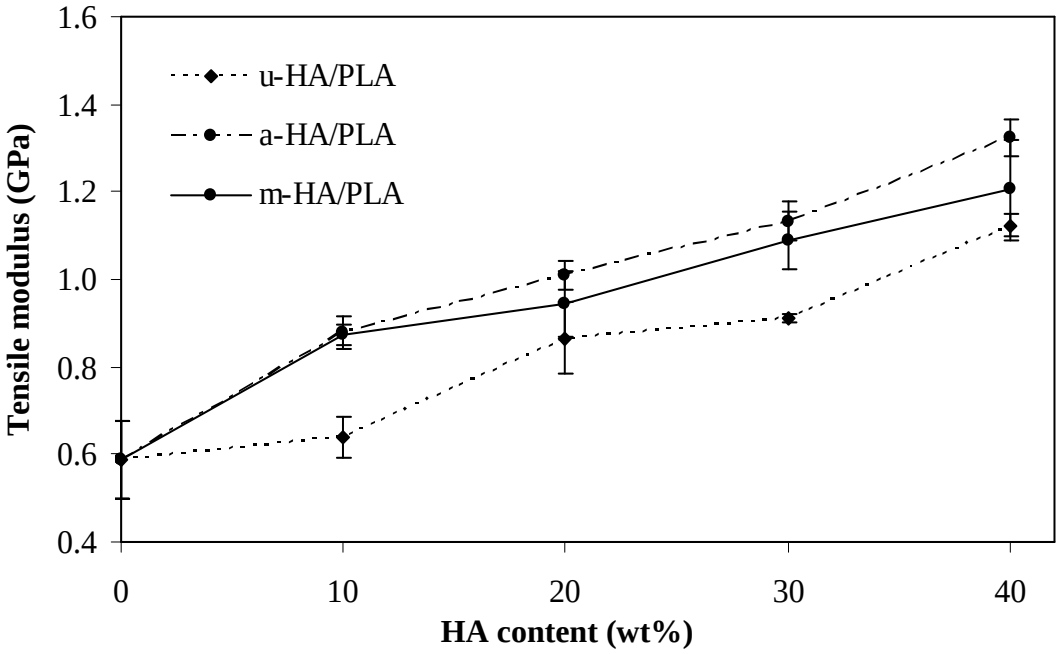

Figure 4.4 Tensile modulus of HA/PLA composites at various HA contents.

Elongation at break of all HA/PLA composites was lower than that of the neat PLA as shown in Figure 4.5. The incorporated HA was the cause of the lower elongation at break of the composites whether or not the HA was surface treated since HA decreased the mobility of PLA chains and led to the decreasing in ductility of the composites. Nevertheless, the PLA composites with silane-treated HA showed higher elongation at break than the corresponding PLA composites with u-HA. This was due to the good dispersion of silane-treated HA in PLA matrix.

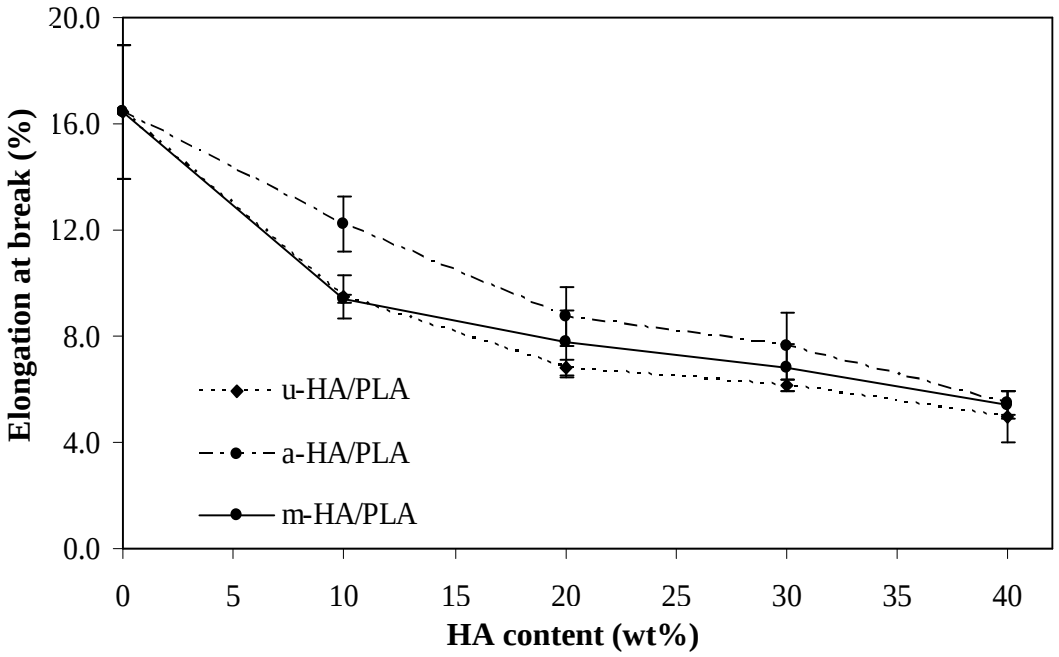

Figure 4.5 Elongation at break of HA/PLA composites at various HA contents.

Tensile strength of HA/PLA composites were slightly lower than that of the neat PLA as shown in Figure 4.6. The tensile strength of the composites continued to decrease with increasing HA content. The decrease in tensile strength of composites with increasing filler content was also observed by other research works (Bleach *et al.*, 2002; Hiljanen, Heino, and Seppala, 1998; Zhongkui *et al.*, 2005). The lowering of tensile strength of the composites was due to the debonding of HA from the polymer matrix by which voids were created (Kasuga *et al.*, 2001; Todo *et al.*, 2006; Takayama *et al.*, 2008). According to this idea, the HA agglomeration observed in tensile fracture surface of HA/PLA composite (Figure 4.8) could be the main reason that was responsible for the reduction in tensile strength of the HA/PLA composites. Nevertheless, the m-HA/PLA composite exhibited the highest tensile strength while the corresponding u-HA/PLA composite show the lowest tensile

strength. This could be attributed to the enhancement of the interaction between HA and PLA as a result of treating HA surface with a silane coupling agent.

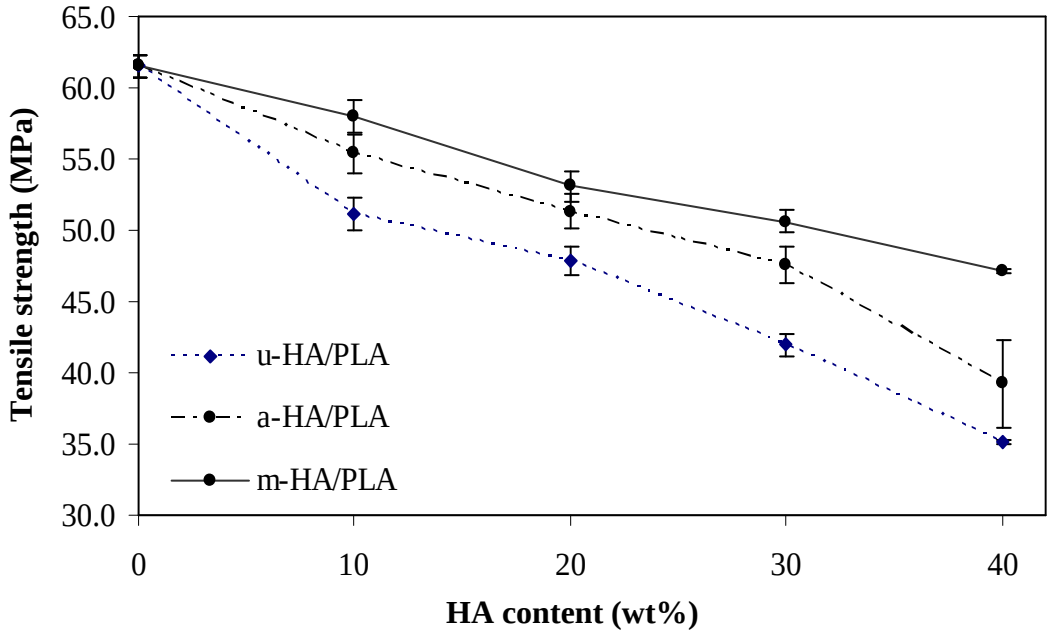

Figure 4.6 Tensile strength of HA/PLA composites at various HA contents.

In cases of m-HA and a-HA/PLA composites, the deposited silane coupling agent on HA surface acted as a bridge between two phases. The most probable reason of the bonding between silane-treated HA and PLA matrix is a degree of solubility of oligomeric siloxanols on HA surface to form interdiffusion and interpenetrating network (IPN) at interphase region (Edwin, 1991). In order to optimize the interfacial interaction, organofunction of the silane coupling agent should be selected to match chemical reactivity, solubility characteristics and structural characteristics of the polymer. Between two types of the silane coupling agent, MPTS exhibited hydrophobic property while APES showed hydrophilic property. Therefore, MPTS was probably more compatible with PLA matrix than

APES. So, m-HA/PLA composite exhibited higher tensile strength than those of u-HA/PLA and a-HA/PLA composites.

Impact strength of HA/PLA composites was attributed to a number of local deformation in the composites. The impact strength of all HA/PLA composites was lower than that of the neat PLA as shown in Figure 4.7. This was because HA disturbed matrix continuity and limited the ability of polymer chains to absorb impact energy. The large agglomerates observed in SEM micrograph of fracture surface of u-HA/PLA composite (Figure 4.8 (a)) were the site of stress concentration, which can act as a microcrack initiator. Moreover, a gap around agglomerated HA indicated the weak PLA-HA interaction. The gap interrupted stress transfer between PLA and HA and led to crack initiation during impact testing. However, the composites with silane-treated HA showed less reduction in impact strength than those with u-HA. Also, the PLA composite containing m-HA showed the highest impact strength. This result was probably due to the better dispersion of the silane-treated HA in PLA matrix.

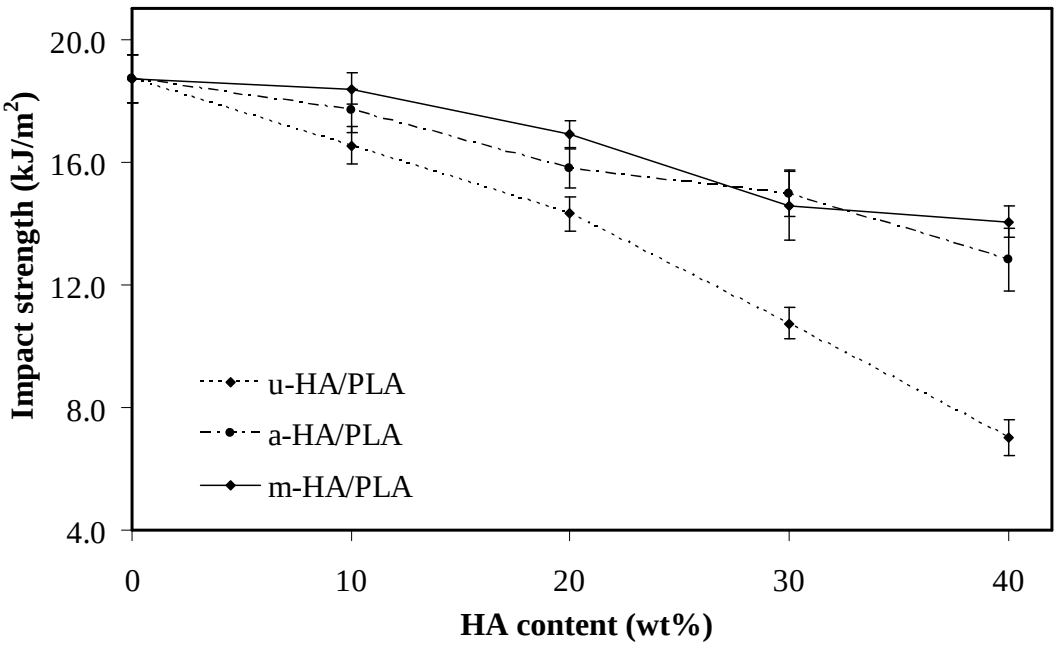

Figure 4.7 Impact strength of HA/PLA composites at various HA contents.

SEM micrographs of tensile fracture surfaces of the HA/PLA composites containing 20wt% of HA are illustrated in Figure 4.8 (a-c). They show that the agglomeration of HA in the PLA phase was found in all types of the PLA composites. Nevertheless, the microstructures of PLA composite containing silane-treated HA in Figure 4.8 (b-c), compared with that of the u-HA/PLA composite in Figure 4.8 (a), illustrated more homogenous dispersion of HA in the PLA matrix with smaller sizes of HA agglomeration. As incorporating HA into PLA, u-HA seemed to have stronger particle-particle interaction than the silane-treated HA. As a result, the u-HA tended to agglomerate during composite processing more than the silane-treated HA did.

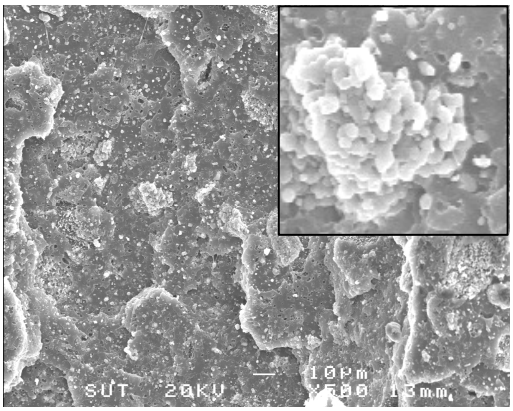

(a)

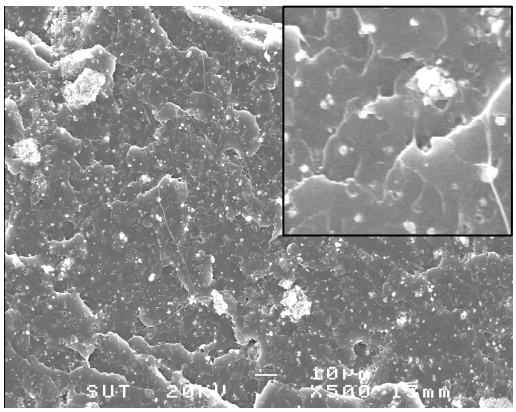

(b)

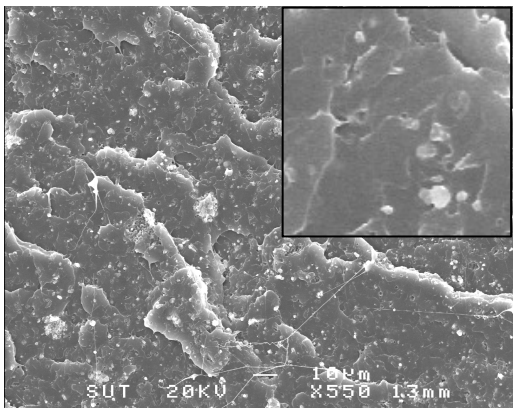

(c)

Figure 4.8 SEM micrographs of tensile fracture surfaces of PLA composites at 20wt% of (a) u-HA, (b) a-HA and (c) m-HA.

In addition, a gap at the interface between u-HA and PLA matrix was observed on the tensile fracture surface of u-HA/PLA composite in Figure 4.8 (a). This revealed local deformation of PLA around these particles. Nevertheless, the gaps between silane-treated HA and PLA interface became smaller as shown in Figure 4.8 (b-c). This suggested that treating HA surface with APES or MPTS can improve interfacial adhesion between PLA and HA. At higher magnifications, as shown in Figure 4.9, silane-treated HA uniformly dispersed within PLA matrixes and closely

adhered to the matrix interface. This result was consistent with the morphology of silane-treated HA shown in Figure 4.3 (c-d).

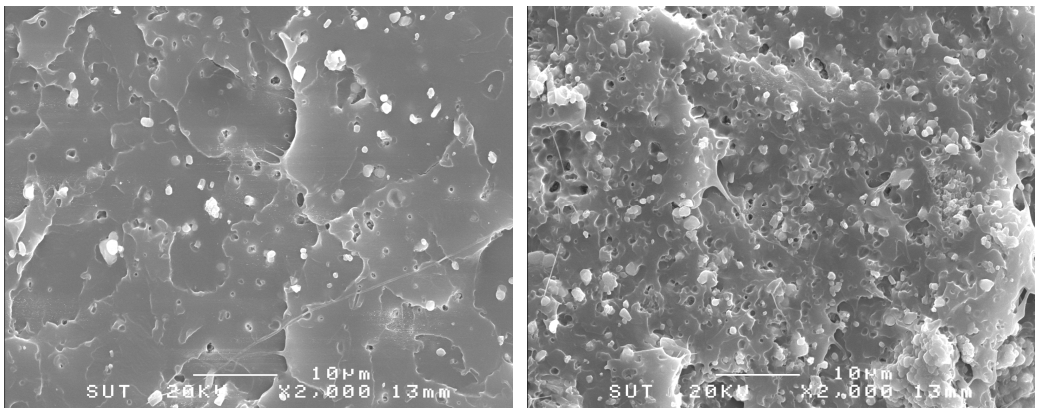

(a) **(b)**

Figure 4.9 SEM micrographs of tensile fracture surfaces at high magnification of composite with m-HA at (a) 10wt% and (b) 40wt%.

4.4.3 *In vitro* cytotoxicity of HA/PLA composites

In order to use the HA/PLA composites in a biomedical application, cytotoxicity and biocompatibility of the composites must be investigated. A preliminary investigation on cytotoxicity of the extracts from HA/PLA composites was performed in this present work. After culturing, the h-OBs cell morphologies were observed. Figure 4.10 (a-g) shows morphologies of the h-OBs cells responded with the reagent control and the extracts from the negative control material, the positive control material, pure PLA and three types of HA/PLA composite specimens, respectively.

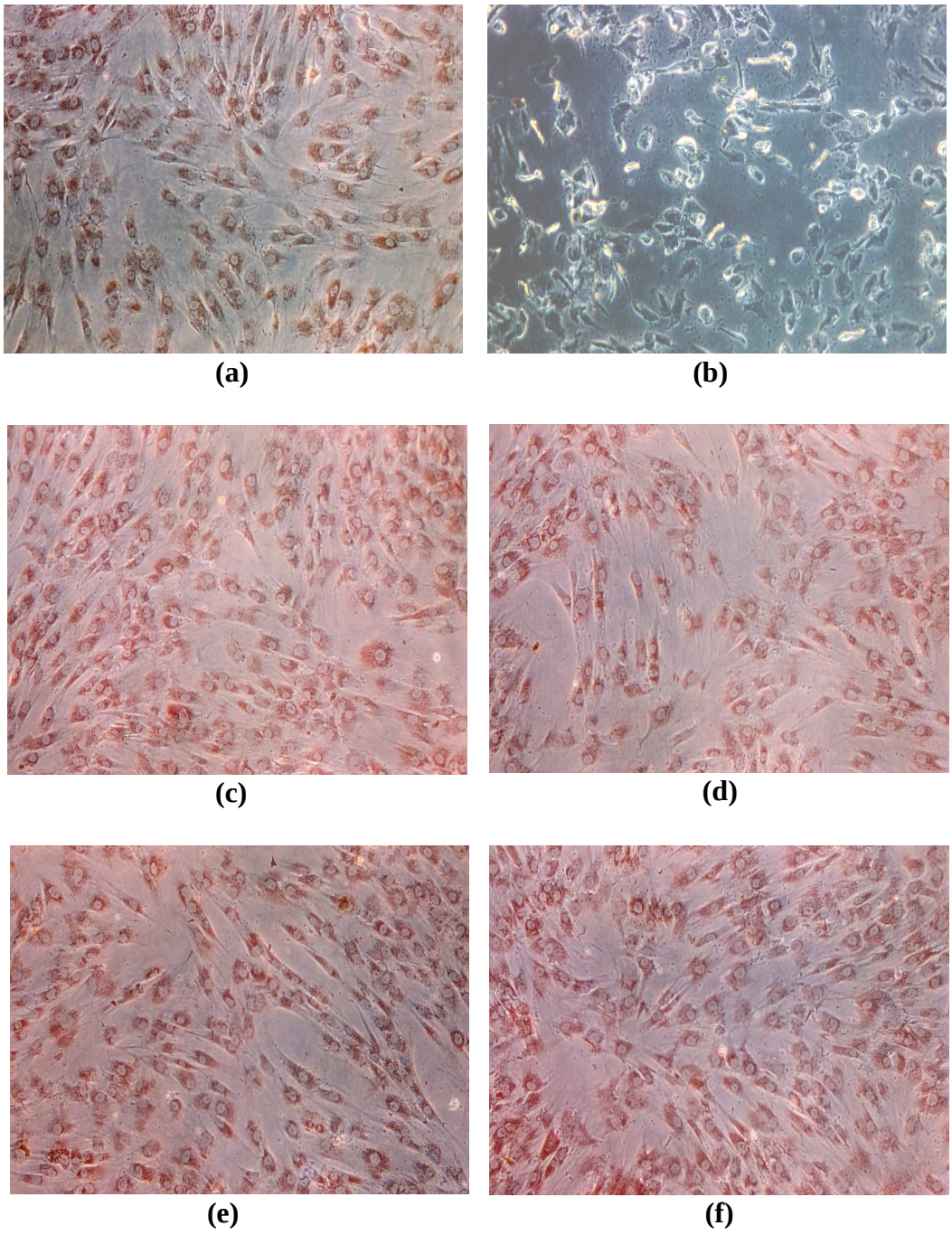

Figure 4.10 Micrographs of h-OBs cells morphology responded with (a) the negative control material extract, (b) positive control material extract, (c) pure PLA extract, (d) u-HA/PLA composite extract, (e) a-HA/PLA composite extract and (f) m-HA/PLA composite extract.

In the negative control material extract (Figure 4.10 (a)), cells morphologies after incubation for 24 h revealed positive staining indicating that these were none cytotoxic (cytotoxicity scale = 0). On the other hand, the h-OBs cells in the positive control material extract exhibited dead cells visible; negative staining was observed (cytotoxicity scale = 3). In addition, Figure 10 (c-f) illustrates morphology of h-OBs cells cultured in the extracts from pure PLA and all types of HA/PLA composites. From the figures, the morphologies of h-OBs cells in the different extracts were similar to those of the reagent control and the negative control material extract. These results demonstrated that u-HA/PLA composite, a-HA/PLA composite and m-HA/PLA composite did not release any substance in the level that was harmful to the h-OBs.

4.5 Conclusions

Preparing biomedical materials from bovine bone is an alternative approach to obtain a suitable bone replacement material with an inexpensive expense. In this study, carbonated HA was produced from thermal treated bovine bone and used as a filler for PLA composites. The results from mechanical test and *in vitro* cytotoxicity test suggested a potential of using bovine bone based HA/PLA composite as a biomaterial. Tensile strength, tensile modulus, elongation at break and impact strength of PLA composites can be improved by modifying u-HA surface with either APES or MPTS. The enhancement of mechanical properties of silane-treated HA/PLA composites was caused by the good dispersion of silane-treated HA in PLA matrix and the good interfacial interaction between the two phases. However, the mechanical

properties of silane-treated HA/PLA composites still need to be enhanced or adjusted in order to meet requirement for a specific medical application.

4.6 References

Benmarouane, A., Hansena, T., and Lodini, A. (2004). Heat treatment of bovine bone preceding spatially resolved texture investigation by neutron diffraction. **Physica B.** 350: 611-614.

Bleach, N. C., Nazhat, S. N., Tanner, K. E., Kellomaki, M., and Tormala, P. (2002). Effect of filler content on mechanical and dynamic mechanical properties of particulate biphasic calcium phosphate-polylactide composites. **Biomaterials.** 23: 1579-1585.

Deng, X., Hao, J., and Wang, C. (2001). Preparation and mechanical properties of nanocomposites of poly(D,L-lactide) with Ca-deficient hydroxyapatite nanocrystals. **Biomaterials.** 22: 2867-2873.

Dupraz, A. M. P., Wijn, J. R., Meer, S. A. T., and Groot, K. (1996). Characterization of silane-treated hydroxyapatite powders for use as filler in biodegradable composites. **J. Biomed. Mater. Res.** 30: 231-238.

Edwin P. P. (1991). **Silane coupling agents.** 2nd ed. New York: Plenum Press; 1991. p. 144-149.

Fathi, M. H., Hanifi, A., and Mortazavi, V. (2008). Preparation and bioactivity evaluation of bonelike hydroxyapatite nanopowder. **J. Mater. Proc. Technol.** 202: 536-542.

Furuzono, T., Sonoda, K., and Tanaka, J.(2001). A hydroxyapatite coating covalently linked onto a silicone implant material. **J. Biomed. Mater. Res.** 56: 9-16.

Hasegawa, S., Ishii, S., Tamura, J., Furukawa, T., Neo, M., Matsusue, Y., Shikinami, Y., Okuno, M., and Nakamura, T. (2006). A 5-7 year *in vivo* study of high-strength hydroxyapatite/poly(L-lactide)composite rods for the internal fixation of bone fractures. **Biomaterials.** 27: 1327-1332.

Hiljanen-Vainio, M., Heino, M., and Seppala, J. V. (1998). Reinforcement of biodegradable poly(ester-urethane) with fillers. **Polymer.** 39: 865-872.

Ignjatovic, N., Suljovrujic, E., Simendic, J. B., Krakovsky, I., and Uskokovic, D. (2001). A study of HAp/PLLA composite as a substitute for bone powder using FT-IR spectroscopy. **Biomaterials.** 22: 271-275.

Kasuga, T., Ota, Y., Nogami, M., and Abe, Y. (2001). Preparation and mechanical properties of Poly(lactic acid) composites containing hydroxyapatite fibers. **Biomaterials.** 22: 19-23.

Kothapalli, C. R., Shaw, M. T., and Wei, M. (2005). Biodegradable HA-PLA 3-D porous scaffolds: Effect of nano-sized filler content on scaffold properties. **Acta Biomater.** 1: 653-662.

Liu, Q., Wijn, J. R., Groot, K., and Blitterswijk, C. A. (1998). Surface modification of nano-apatite by grafting organic polymer. **Biomaterials.** 19: 1067-1072.

Ooi, C. Y., Hamdi, M., and Ramesh, S. (2007). Properties of hydroxyapatite produced by annealing of bovine bone. **Ceram. Int.** 33: 1171-1177.

Ruksudjarit, A., Pengpat, K., Rujijanagul, G., and Tunkasiri, T. (2008). Synthesis and characterization of nanocrystalline hydroxyapatite from natural bovine bone. **Curr. Appl. Phys.** 8: 270-272.

Russias, J., Saiz, E., Nalla, R. K., Gryn, K., Ritchie, R. O., and Tomsia, A. P. (2006). Fabrication an mechanical properties of HA/PLA composites:A study of *in vitro* degradation. **Mater. Sci. Eng. C.** 26: 1289-1295.

Shikinami, Y. and Okuno, M. (2001). Bioresorbable devices made of forged composites of hydroxyapatite (HA) powders and poly L-lactide (PLLA). Part II: practical properties of miniscrews and miniplate. **Biomaterials**. 22: 3197-3211.

Shinzato, S., Nakamura, T., Kokubo, T., and Kitamura, Y. (2001). Bioactive bone cement: Effect of silane treatment on mechanical properties and osteoconductivity. **J. Biomed. Mater. Res.** 55: 277-284.

Takayama, T., Todo, M., and Takano, A. (2008). The effect of bimodal distribution on the mechanical properties of hydroxyapatite particle filled poly(L-lactide) composites. **J. Mech. Behav. Biomed. Mater.** 2: 105-112.

Todo, M., Park, S. D., Arakawa, K., and Takenoshita, Y. (2006). Relationship between microstructure and fracture behavior of bioabsorbable HA/PLLA composites. **Composits: Part A.** 37: 2221-2225.

Tsuji, H. and Ikarashi, K. (2004). *In vitro* hydrolysis of poly(lactide) crystalline residues as extended-chain crystallites. Long-term hydrolysis in phosphate-buffered solution at 30ºC. **Biomaterials.** 25: 5449-5455.

Wen, J., Li, Y., Zuo, Y., Zhou, G., Li, J., Jiang, L., and Xu, W. (2008). Preparation and characterization of nano-hydroxyapatite/silicone rubber composite. **Mater. Lett.** 62: 3307-3309.

Yoganand, C. P., Selvarajan, V., Wu, J., and Xue, D. (2009). Processing of bovine hydroxyapatite (HA) powders and synthesis of calcium phosphate silicate glass ceramics using DC thermal plasma torch. **Vacuum.** 83: 319-325.

Zhang, S. M., Liu, J., Zhou, W., Cheng, L., and Guo, X. D. (2005). Interfacial fabrication and property of hydroxyapatite/polylactide resorbable bone fixation long-term composite. **Curr. Appl. Phys.** 5: 516-518.

Zhongkui, H., Peibiao, Z., Chaoliang, H., Xueyu, Q., Aixue, L., Li, C., Xuesi, C., and Xiabin, J. (2005). Nano-composite of poly(L-lactide) and surface grafted hydroxyapatite: Mechanical properties and biocompatibility. **Biomaterials.** 26: 6296-6304.